On the Modeling of Losses in Short Length Photonic Crystal Waveguides

Martin J. Cryan

***Abstract*—The 3-D finite difference time domain (FDTD) cut-back method is used to study losses in nondisordered photonic crystal silicon membrane waveguides. Losses above the light-line have been shown to be in good agreement with other methods. Below the light-line, however, FDTD is predicting a rapid increase in losses. This paper studies the possible causes for this effect, including meshing effects, back reflections, and finite thickness sidewalls. It is found that since below the light-line the group index becomes very high and the loss becomes very low, strong Fabry–Perot oscillations dominate the cut-back results. The paper also discusses the impact of operating near to the cut-off wavelength of the photonic crystal waveguide Bloch mode and the implications this has for loss calculation.**

***Index Terms*—Photonic crystals.**

I. Introduction

LOSSES in PhC waveguides have been studied for a number of years. Recently great progress has been made in reducing loss levels in membrane waveguides to <1 dB/mm [1], [2]. It has been realized that even when working below the light-line it is difficult to maintain low loss over large bandwidths. Much work, both experimental and theoretical has studied this regime and in particular the role of disorder [3]–[6]. It is, however, interesting to consider the much simpler case of a completely uniform waveguide with no disorder as a benchmark against which to assess the effects of disorder. When modeling such a system with purely modal, frequency domain methods [4], [7], [8], the loss must be zero below the light-line; however, somewhat unexpectedly, other nonmodal methods produce finite losses below the light-line [9], [10]. Obviously, this must be an extrinsic loss since theoretically there must be no loss below the light-line. Experimentally, groups have observed increasing loss below the light-line which is postulated to be caused by roughness induced scattering being increased by the low group velocity regime [4], [11]. However, in the case of the aforementioned modeling results [9], [10], there is no disorder, and, thus, a different explanation is required. This paper will study the uniform, nondisordered waveguide case and look at the possible reasons why such increasing losses could occur including, meshing effects, back reflections and finite thickness sidewalls. This is then followed by a detailed assessment of power flows from the structure including both sidewall and out-of-plane leakage. There is then a discussion on the role of Fabry–Perot oscillations in the cut-back method and its impact on accuracy. Finally comments are made on the fact that the cut-off wavelength for the Bloch mode in the PhC waveguide is within the spectral region being studied here.

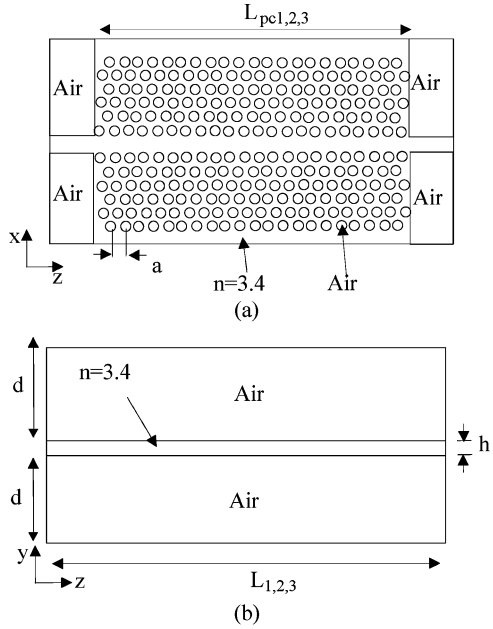

Fig. 1. Photonic crystal membrane waveguide with $r/a = 0.3$, $a = 430.55$ nm, $h = 0.6a = 258.3$ nm, $L_{1,2,3} = 6.028\,\mu$m, $10.76\,\mu$m, 19.37μm, $L_{pc1,2,3} = 11a, 22a, 42a$, $d = 870$ nm, W1 guide in $\Gamma - K$ direction, $n = 3.4$ (a) top view, (b) side view.

II. Simulation Results and Discussions

Fig. 1 shows the structure to be studied. This is a silicon slab PhC waveguide with dimensions that have been used in a number of earlier works [8], [12]. It was also the subject of a benchmarking exercise in the EU COST-P11 activity on PhCs [13]. The band structure of this structure has been extensively studied [14]–[16] and the membrane is found to support an even and odd TE-like mode (E parallel to slab). This work concentrates solely on the even TE-like mode, since this is the most commonly used.

Losses are calculated using the FDTD cut-back method as described in [12]. The structure has uniform meshing in the $x - z$ plane, with $\Delta x = 20.15$ nm and $\Delta z = 21.53$ nm. This results in 20 cells per lattice constant, a, in the z direction and 37

Manuscript received February 10, 2009; revised June 17, 2009 and July 21, 2009. First published July 31, 2009; current version published September 10, 2009.

The author is with the Department of Electrical and Electronic Engineering, University of Bristol, Bristol, BS8 1UB, U.K. (e-mail: m.cryan@bristol.ac.uk).

Color versions of one or more of the figures in this paper are available online at http://ieeexplore.ieee.org.

Digital Object Identifier 10.1109/JLT.2009.2028658

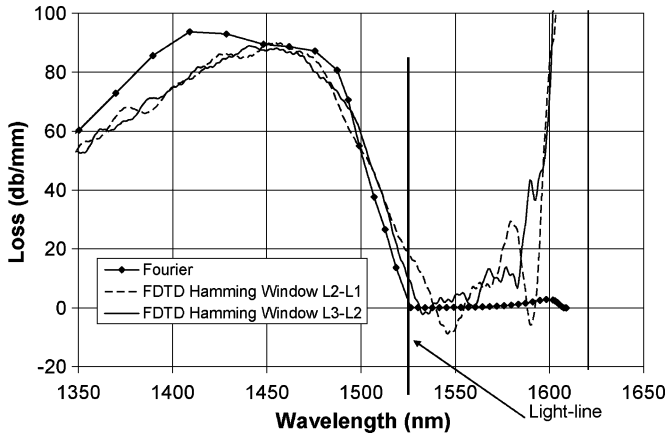

Fig. 2. FDTD and Fourier method simulated loss results for waveguide shown in Fig. 1.

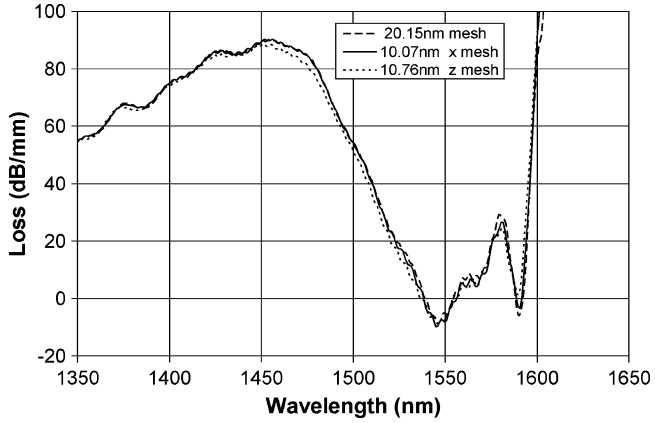

Fig. 3. Losses for different FDTD mesh sizes in both x and z directions.

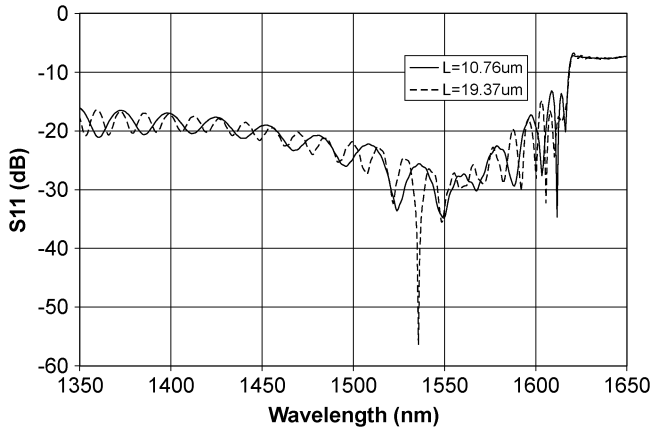

Fig. 4. Modal back reflection for two different length PhC waveguides.

cells per $\sqrt{3}a$ in the x direction. This produces uniform meshing across the holes and keeps staircasing errors constant across the structure. In the vertical direction, nonuniform meshing is used with a $\Delta y_{\min} = 16.14$ nm, resulting in 16 cells in the membrane. PhC waveguide L_3 results in a simulation requiring 800 MB of RAM and taking 140 h on a Pentium 4 2.4-GHz machine. This method uses modal S-parameters to accurately calculate transmission through three different length waveguides and from this, loss per unit length data can be calculated. In these simulations great care has been taken to remove any artificial roughness that can be introduced by staircasing caused by the FDTD grid. Thus, although the holes will not be perfectly circular, they will all be identical and arrayed perfectly periodically. Later in this paper the effects of this residual staircased roughness will be studied. Hamming windowing of the time domain data is used to remove residual ringing effects [12]. Fig. 2 presents loss in dB/mm versus wavelength obtained from the FDTD cut back method and from a Fourier Modal method [8]. It shows that good agreement is obtained above the light-line from 1350–1525 nm; however, as discussed above, the Fourier modal method predicts very small losses below the light-line. The FDTD results on the other hand show rapidly increasing losses. These have been observed, but not commented on using another nonmodal method namely the Multiple Scattering Technique [9]. It should be noted that Fig. 2 shows negative losses which are obviously unphysical and to remove these would need longer length guides. Thus, there is a limit to the accuracy of these results of around $+/-10$ dB/mm. However, for the purposes of this paper where very large losses are being observed below the light-line this level of accuracy is sufficient. This paper will now investigate possible reasons for these increasing losses as discussed in the introduction.

In any numerical method such as FDTD which relies on meshing the most important effect to observe is the dependence of the results on mesh size. As the mesh size is reduced the results should converge to some limit. Care should be taken here since reducing the mesh size results in reduced time step size which can make comparison of results less straightforward. Fig. 3 shows these results for the case when the x direction mesh is reduced from 20.15 to 10.07 nm and the z direction mesh is reduced from 21.53 m to 10.76 nm. Due to memory constraints it was not possible to refine the mesh in both x and z directions simultaneously. It can be seen that the results remain almost constant. Not only does this show the method is converged but also that any numerical surface roughness effects caused by staircasing are not inducing the loss below the light-line.

The following results look at the effects of back reflection, which occurs in any low group velocity waveguide due to both increased modal mismatch and group velocity mismatch. If the back reflection was increasing with the length of waveguide, as might be expected in say a 1-D Distributed Bragg Reflector(DBR) structure then the cut-back method used here would produce finite loss results since it is assuming fixed reflection loss at each transition. The back reflection can be calculated directly by the FDTD method outlined above : since the input photonic waveguide is being excited by its fundamental mode, almost all of the energy is directed forwards; thus, any energy observed behind the excitation point must be due to back reflection. Thus, a modal time domain probe is placed before the excitation and this calculates the amount of power reflected back into the fundamental mode of the input waveguide. The results for two different length guides are shown in Fig. 4.

Fig. 4 shows that apart from a change in interference beat period due to the change in length no extra back reflection appears to be occurring. It remains a possibility that energy is

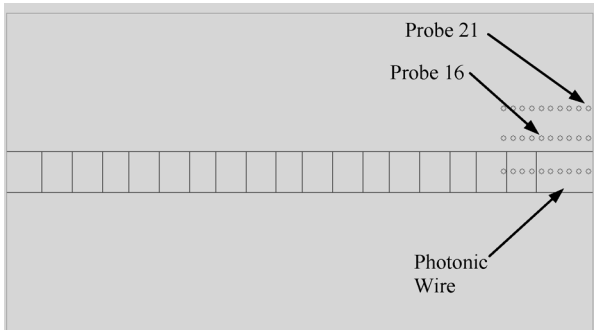

Fig. 5. View of probe positions for assessing reflection into higher order modes.

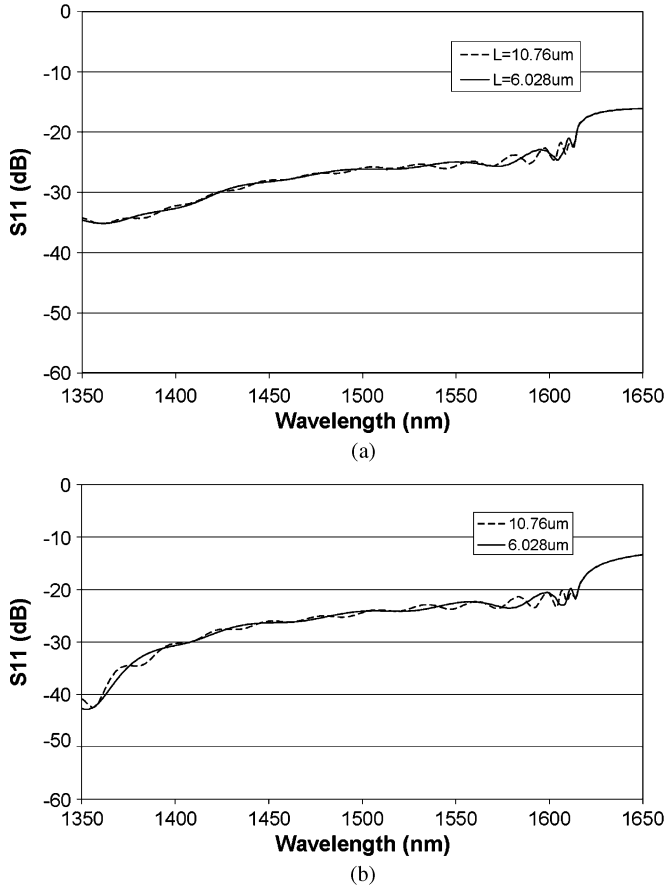

Fig. 6. Total back reflected power at (a) probe 21 and (b) probe 16 from different length waveguides.

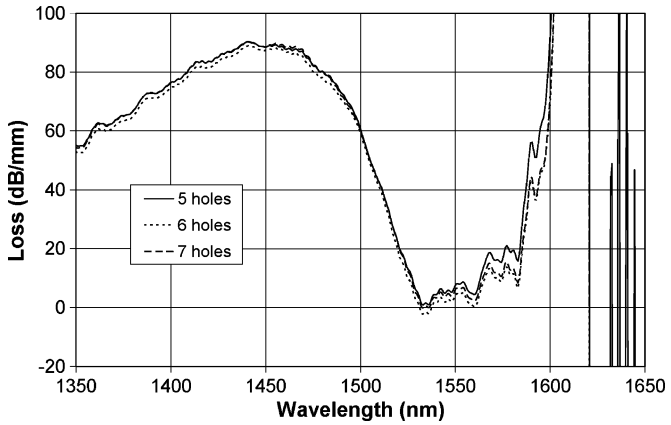

Fig. 7. Loss dependence on number of rows of holes in PhC waveguide sidewall.

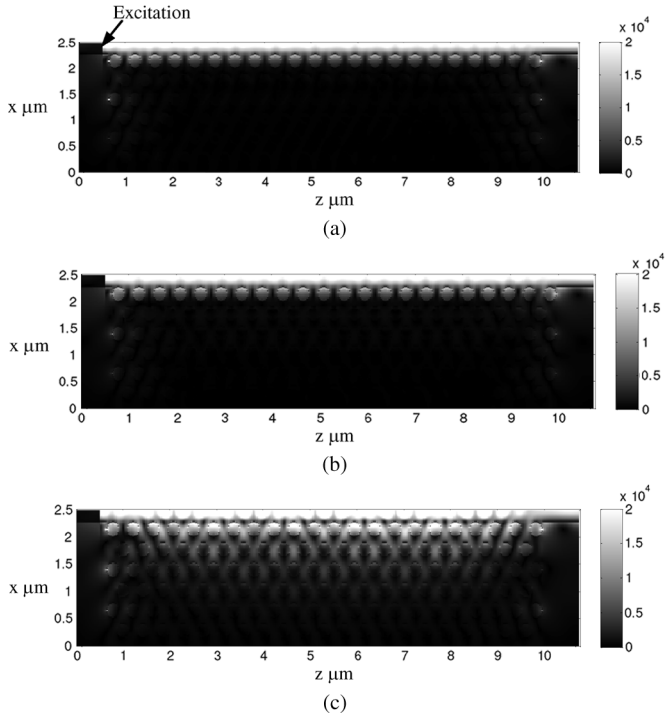

Fig. 8. Field plots for abs (E_x) at center of slab—top view for wavelength (a) 1.475μm, (b) 1.525 μm, (c) 1.6 μm.

being reflected back into higher order modes of the waveguide. Currently overlap integrals cannot be performed with respect to higher order modes, so in order to assess this effect, standard time domain probes are placed around the input photonic wire to assess the reflection into other modes. The probe positions are shown in Fig. 5 which is a view taken from the FDTD user interface.

Example probes, shown as probe numbers 21 and 16 are used to sample the back reflected energy. The results are shown below in Fig. 6 and they confirm that there is no strong dependence on length in this case either.

Low group velocity can increase existing loss because the light takes longer to propagate through the waveguide. Thus, it could be postulated that sidewall leakage is being increased by the low group velocity. To study this effect, different thickness side walls have been studied by increasing and decreasing the number of rows of holes in the sidewalls. Fig. 7 shows these results. It can be seen that there is a small dependence on number of rows of holes in the sidewall, however, these results alone seem not to explain the dramatic rise below the light-line.

Thus, to understand in detail where power is being lost from the structure the fact that FDTD has access to all fields in the simulation domain can be used [14]. Thus, power leaking vertically from the structure can be calculated. In order to do this a measurement plane can be placed above the slab a distance of 0.47 μm from the surface of the slab. In this code these measurement planes can be specified in the frequency domain where a running discrete Fourier transform is performed at each point in

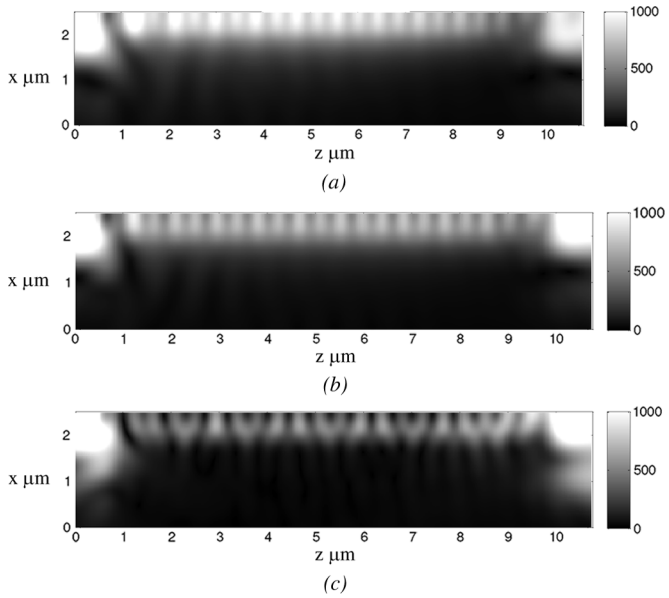

Fig. 9. Field plots of abs (E_x) 0.47 μm above the slab—top view for wavelength (a) 1.475 μm, (b) 1.525 μm, (c) 1.6 μm.

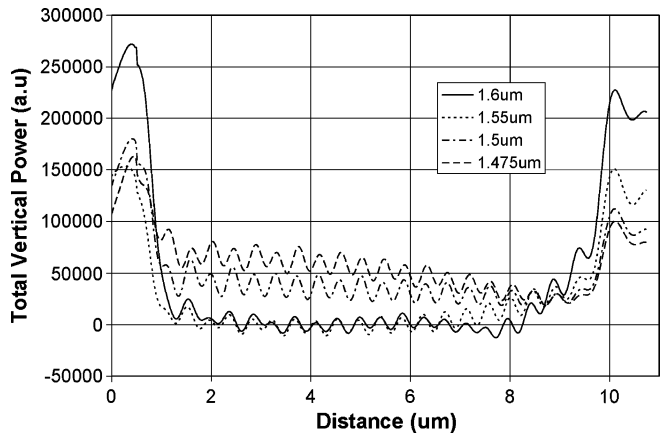

Fig. 10. Total vertical power versus distance for different wavelengths.

the plane at a specified frequency. First, however, it is instructive to observe the field profiles at the center of the slab at three different wavelengths, above (1.475 μm), close to (1.525 μm) and below (1.6 μm) the light-line.

These show the strong confinement that can be achieved in these types of waveguide and that in (c) below the light-line the mode is more extended as expected in a low group velocity regime and has high fields in the holes nearest to the guide. Note also that most of the energy is propagating to the right of the excitation point—indicating forward propagation, this is what enables the reflection calculation carried out previously. Now the electric field is observed 0.47 μm above the slab in Fig. 9.

Here, we can see that substantial amount of energy is present in this plane and as expected below the light-line much less power is present, though the total amount of power is not clear from looking at only the E_x field. Thus, the Poynting vector at each z value in this plane has been summed and can be plotted versus distance for each wavelength as shown in Fig. 10.

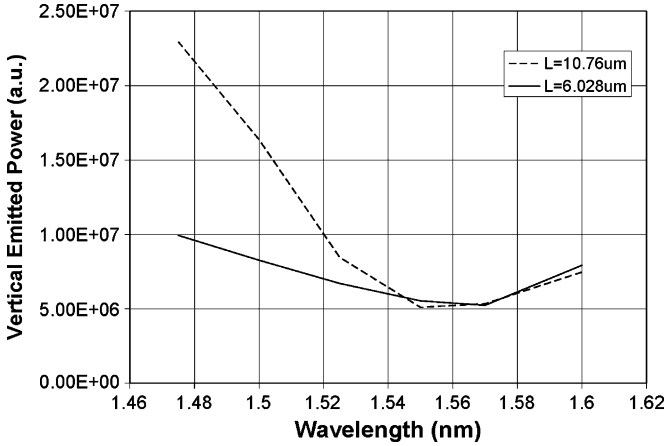

Fig. 11. Total vertically emitted power at different wavelengths for different length guides.

There are a number of interesting features in Fig. 10. Firstly it can be seen that for wavelengths above the light-line the out of plane leakage is high as expected. Below the light-line the out of plane leakage is much smaller, in fact on close inspection of Fig. 10 it can bee seen that below the light-line power is in fact travelling in both the positive and negative vertical direction, this is indicative of evanescent near fields which are not leaking in the vertical z direction. Another interesting feature is the large amount of power being scattered at the input and output of the waveguide. This will be mostly due to the transition from the photonic wire waveguide to PhC waveguide. It can be seen that the amount of scattering is increasing as the wavelength moves further below the light-line, as expected since both the modal and group velocity mismatch are increasing.

In order to further quantify the vertical leakage below the light-line, the analysis of Fig. 10 can be repeated for a different length guide—6.028 μm in this case. The total vertically emitted power can then be summed at each wavelength and plotted as shown in Fig. 11.

Fig. 11 shows that above the light-line the total vertically emitted power is increasing with length as would be expected. However, below the light-line, there is no length dependence, and, thus, this must be pure end effect loss.

Thus, this section has confirmed as expected there is no vertical leakage from these waveguide below the light-line.

The paper will now consider the case of sidewall leakage. This has been studied in 2-D models [17], [18] but less so in full 3-D with a focus on below light-line operation. The following results show a Poynting vector calculation for sidewall leakage. Thus, frequency domain snapshots are placed as shown in Fig. 12 below.

In this case different thickness sidewalls will be studied as in Fig. 7. Fig. 13 shows the x directed Poynting vector at 1.6 μm for 7, 6 and 5 hole thick sidewalls.

The results in Fig. 13 show very convincingly that sidewall leakage is a strong function of sidewall thickness. The results can be used to calculate total sidewall leakage at different wavelengths, these results are summarized in Fig. 14.

Fig. 14 furthers confirms that sidewall leakage is strongly dependent on the thickness of the walls and also on the wavelength

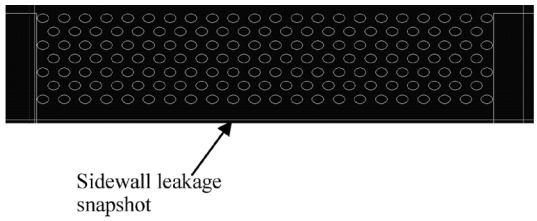

Fig. 12. Top view of sidewall leakage snapshot in 7 hole thick sidewall case.

once propagation is below the light-line. These results suggest that the loss below the light-line observed in Fig. 2 could be caused by sidewall leakage being enhanced by low group velocity. The ultimate test of this is to further increase the sidewall thickness to attempt to eliminate side wall loss. Fig. 15 shows a PhC waveguide with very thick sidewalls. The cut back method has again been used here with two different length waveguides in order to extract the loss.

The loss result for this structure is shown below in Fig. 16 and it is clear that the loss below the light-line is still present, implying that sidewall leakage is not the cause of the observed increasing losses.

Thus, at this point, the paper has shown that the loss observed below the light-line could be nonphysical in nature and may be due to the cut back method itself. The length of waveguides being used here are very short when compared to typical lengths used in measurement based cut-back methods, however, above the light-line reasonable results are being obtained. Thus, it is in the low group velocity regime that the cut-back method starts to breakdown. Below the light-line this waveguide becomes essentially lossless apart from small levels of sidewall loss. Thus, in terms of the cut back method if the z directed Poynting vector is measured at any point in the waveguide it should be essentially unchanged, resulting in zero loss. This can be tested directly here by placing modal time probes along the waveguide as shown in Fig. 17. These are modal overlap integrals with respect to the fundamental mode of the input waveguide and, thus, will only approximate the actual z-directed Poynting vector of the Bloch mode that exists in the PhC waveguide. However, these would still be expected to be essentially constant in a lossless waveguide. The results are normalized to the straight photonic wire waveguide case and, hence, are termed transmission coefficients (S21).

Fig. 18 shows the results for the time probes at three different positions. A number of features are observed. Firstly the snapshots near the input of the waveguide are seen to be larger in magnitude above the light-line than those nearer the output, as might be anticipated in a lossy waveguide. Secondly, the Fabry–Perot ripple increases in period as the probe moves to the output again as expected since the probe is moving closer to the mismatch at the output of the waveguide. It is clear that as the wavelength goes below the light-line the Fabry–Perot effects start to increase dramatically in amplitude, due to the fact that losses in the waveguide have become very low. There is also an overall increase in the average level of the transmission coefficient, this is indicative of the increase field intensity that occurs in the slow light regime which gives rise to enhanced nonlinear performance in these types of waveguide. The period

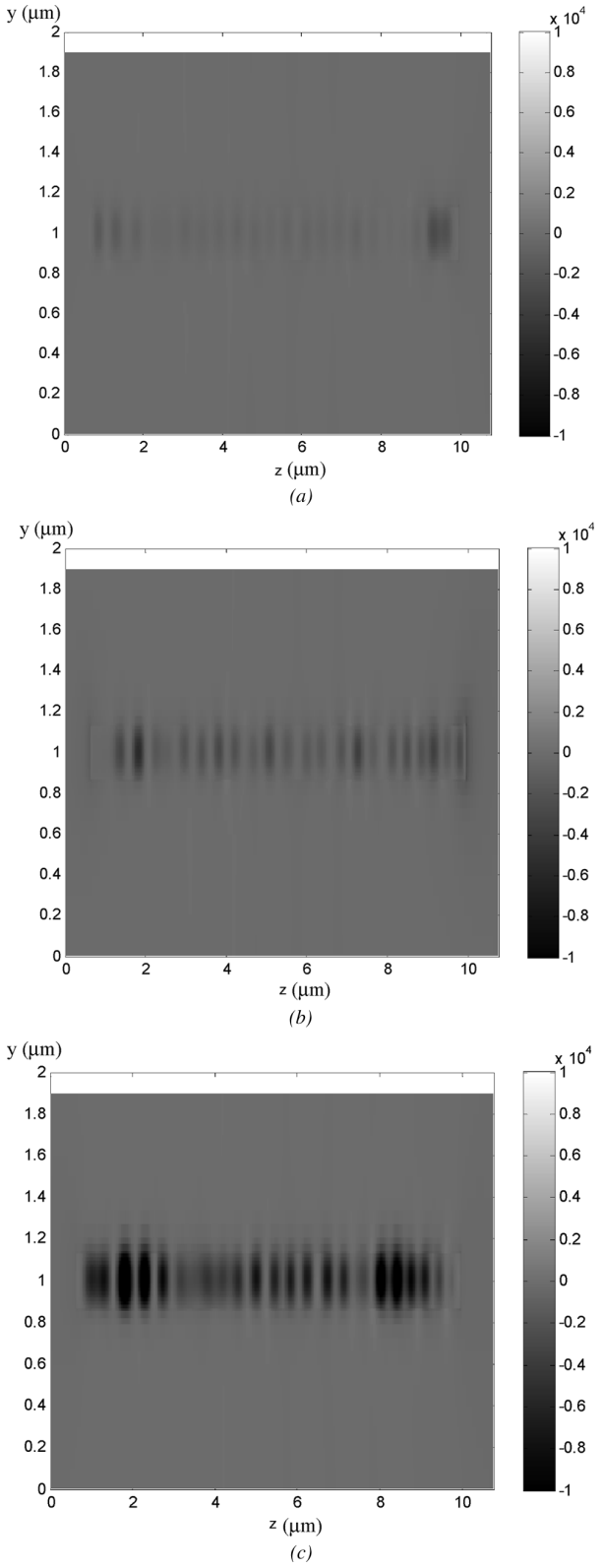

Fig. 13. Side view of x directed Poynting vector at 1.6 μm in snap plane shown in Fig. 12, for (a) seven hole, (b) six hole, and (c) five hole thick side walls. The slab extends from 0.871 μm to 1.129 μm in the y direction.

of oscillation also starts to rapidly decrease as the group index of the waveguide is increasing and, thus, increasing the effective length of the waveguide. The cut back method relies on taking differences between time probes in different length waveguides,

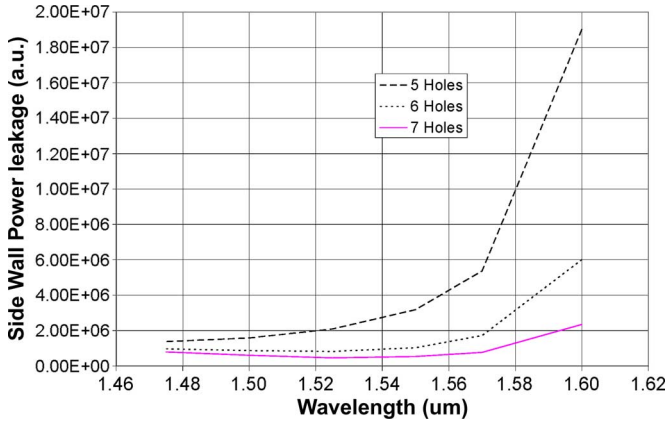

Fig. 14. Total sidewall leakage versus wavelength for different thickness sidewalls.

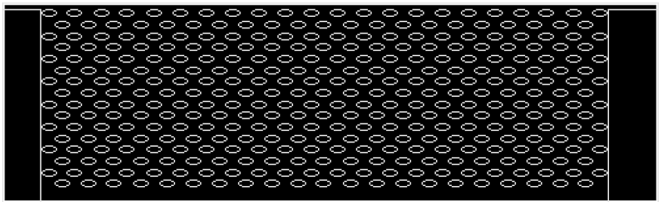

Fig. 15. PhC waveguide with very thick (16 rows) sidewalls to strongly reduce sidewall leakage.

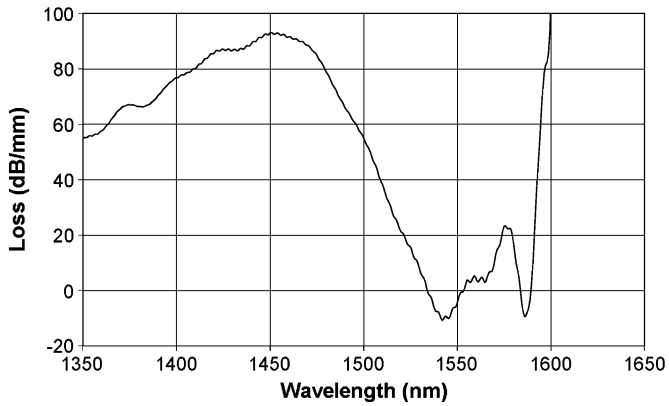

Fig. 16. PhC waveguide with very thick sidewalls (16 rows) to strongly reduce sidewall leakage.

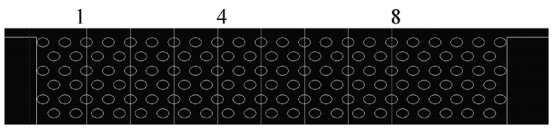

Fig. 17. PhC waveguide with modal time probes distributed along its length, showing positions 1, 4, and 8.

and, thus, these results show that it becomes very susceptible to errors in the low group velocity regime.

In order to explore the effect of Fabry–Perot ripples it is important to increase the frequency domain resolution in these results. Currently Hamming windowing is being used to reduce ringing caused by the finite length time sample being taken. Thus, here the simulation is extended from 65535 to 120000 time points.

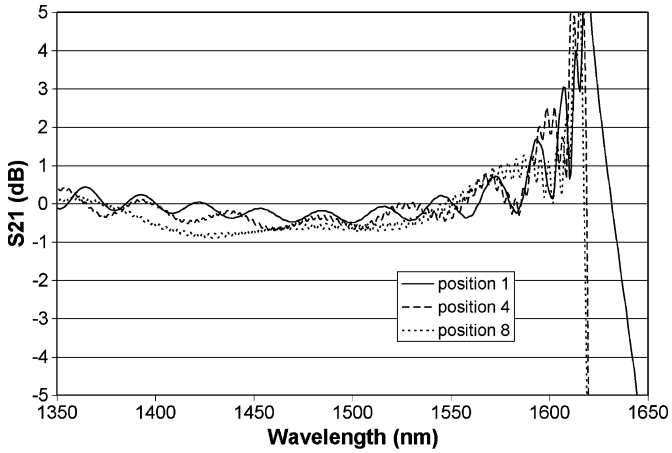

Fig. 18. Normalized overlap integral at different positions down the PhC waveguide.

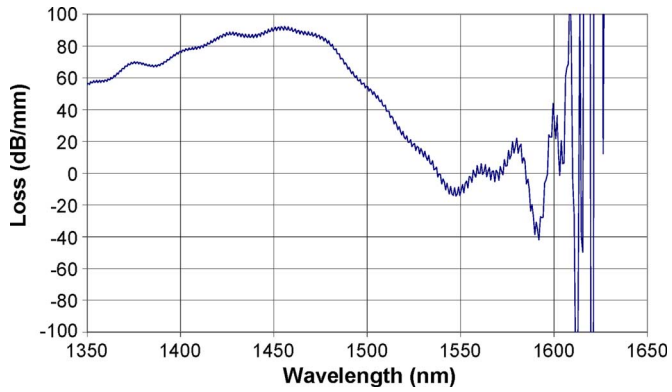

Fig. 19. Loss for L2-L1 for 120-K time points with no Hamming windowing.

Fig. 19 shows that with the increased number of time points, the ringing effect has been reduced to a very fast, small amplitude ripple observed across the whole spectrum (see [12] for unwindowed results at 65536 time points). In contrast to the previous results, however, the fine detail beyond 1600 nm is now more visible. It is very clear that a strong ripple is being observed here, which after windowing was not being resolved. This appears to confirm that an important issue here is one of Fabry–Perot oscillation introducing inaccuracy when comparing the transmission of different length guides. However, what is also clear from Fig. 19 is that there remains an increasing trend to the loss results below the light line. One important point that has yet to be discussed is the fact that PhC waveguides such as this can become cut-off at a particular wavelength [14]–[16], [19] such that there are no modes available to transport energy and the modes become purely evanescent. A strong indication for the onset of this regime is given in Fig. 4 where the reflection coefficient changes from a periodically varying response to a constant high level at 1620 nm. This would agree with the idea that a large portion of the input energy is being reflected directly from the input of the waveguide and a small amount is evanescently coupling into the waveguide. Thus, there will be no signal being reflected from the output to cause the Fabry–Perot oscillation. A cut-off waveguide is well know to act as a strong attenuator and it

appears that the increasing loss observed here may indeed by physical and be associated with a transition from propagating to evanescent modes. Fig. 19 also shows nonphysical results in that gain is being observed. This is caused by Fabry–Perot ripple in the longer length waveguide causing the transmission to sometimes go above that of the shorter guide. This situation can be improved by using larger numbers of longer length waveguides.

III. Conclusion

This paper has explored the large losses observed in PhC waveguides below the light-line when using the FDTD cut-back method. Above the light-line where the group velocity is "normal" and losses are high, very good agreement with other methods is obtained. However, below the light-line where losses are very low and the group index is very high, large amplitude Fabry–Perot ripples observed in the transmission response reduce the accuracy of the method. By increasing the frequency resolution of the method with increased number of time points the effect of the Fabry–Perot ripples has been more clearly observed. Beyond this regime this paper discusses the impact of the proximity of the cut-off wavelength for the Bloch mode in the PhC waveguide. It appears that the increasing loss may be in part due to a transition from a propagating to an evanescent mode in the waveguide. It should be noted that frequency domain methods such as the Fourier Modal Method shown in Fig. 2 do not, unlike the FDTD method, in general include evanescent modes; hence, the large discrepancy with FDTD based results below the light-line. Workers studying the impact of disorder below the light-line may need to take into account that even in this completely ordered, lossless case quite complex behavior is observed. Future work will use longer waveguide lengths and tapers to improve the understanding of these results.

Acknowledgment

The author would like to thank Prof. Railton and Prof. Craddoock for their work in developing the FDTD code used here, and Prof. J. McGeehan for the use of the Condor computing cluster which was donated to the Department of Electrical and Electronic Engineering by Toshiba Research Labs Europe. He would also like to thank P. Wade and P. Townsend who implemented and maintain the cluster, as well as the reviewers for constructive comments.

References

[1] E. Dulkeith, S. J. McNab, and Y. A. Vlasov, "Mapping the optical properties of slab-type two-dimensional photonic crystal waveguides," *Phys. Rev. B*, vol. 72, p. 115102, 2005.

[2] Y. Sugimoto, Y. Tanaka, N. Ikeda, Y. Nakamura, K. Asakawa, and K. Inoue, "Low propagation loss of 0.76 dB/mm in GaAs-based single-line-defect two-dimensional photonic crystal slab waveguides up to 1 cm in length," *Opt. Exp.*, vol. 12, pp. 1090–1096, Mar. 2004.

[3] S. Hughes, L. Ramunno, J. F. Young, and J. E. Sipe, "Extrinsic optical scattering loss in photonic cristal waveguides: Role of fabrication disorder and photon group velocity," *Phys. Rev. Lett.*, vol. 94, p. 033903, 2005.

[4] L. C. Andreani and D. Gerace, "Light-matter interaction in photonic crystal slabs," *Phys. Stat. Sol. (B)*, vol. 244, no. 10, pp. 3528–3539, 2007.

[5] J.-M. Brosi, J. Leuthold, and W. Freude, "Microwave-frequency experiments validate optical simulation tools and demonstrate novel dispersion-tailored photonic crystal waveguides," *IEEE J. Lightw. Technol.*, vol. 25, no. 9, Sep. 2007.

[6] L. O'Faolain, T. P. White, D. O'Brien, X. Yuan, M. D. Settle, and T. F. Krauss, "Dependence of extrinsic loss on group velocity in photonic crystal waveguides," *Opt. Exp.*, vol. 15, no. 20, pp. 13129–13138, October 2007.

[7] P. Lalanne, "Electromagnetic analysis of photonic crystal waveguides operating above the light cone," *IEEE J. Quant. Electron.*, vol. 38, no. 7, pp. 800–804, Jul. 2002.

[8] C. Sauvan and P. Lalanne *et al.*, "Accurate modeling of line-defect photonic cristal waveguides," *IEEE Photon. Technol. Lett.*, vol. 15, no. 9, pp. 1243–1245, Sep. 2003.

[9] S. Boscolo and M. Midrio, "3D multiple-scattering technique for the analysis of photonic crystal Slabs," *J. Lightw. Technol.*, Dec. 2004.

[10] M. J. Cryan, I. J. Craddock, and C. J. Railton, "FDTD modelling of losses and group velocity below the light-line in PhC Slabs," presented at the Photonic and Electromagnetic Crystals Conf., PECS VI, Crete, Greece, Jun. 2006.

[11] Y. Tanaka, Y. Sugimoto, N. Ikeda, H. Nakamura, K. Asakawa, K. Inoue, and S. G. Johnson, "Group velocity dependence of propagation losses in single-line-defect photonic crystal waveguides on GaAs membranes," *Electron. Lett.*, vol. 40, no. 3, Feb. 5, 2004.

[12] M. J. Cryan, D. C. L. Wong, I. J. Craddock, S. Yu, J. Rorison, and C. J. Railton, "Calculation of losses in 2D photonic crystal membrane waveguides using the 3D FDTD method," *IEEE Photon. Technol. Lett.*, vol. 17, no. 1, pp. 58–60, Jan. 2005.

[13] COST P11: The Physics of Linear, Non-linear and Active PhCs [Online]. Available: http://w3.uniroma1.it/energetica/copy.htm, http://w3.uniroma1.it/energetica/WG2.htm

[14] W. Kuang, C. Kim, A. Stapleton, W. J. Kim, and J. D. O'Brien, "Calculated out-of-plane transmission loss for photonic-crystal slab waveguides," *Opt. Lett.*, vol. 28, no. 19, pp. 1781–1783, Oct. 1, 2003.

[15] M. Notomi, K. Yamada, A. Shinya, J. Takahashi, C. Takahashi, and I. Yokohama, "Extremely large group-velocity dispersion of line-defect waveguides in photonic crystal Slabs," *Phys. Rev. Lett.*, vol. 87, no. 25, p. 253902, Dec. 17, 2001.

[16] A. Sugitatsu and S. Noda, "Room temperature operation of 2D photonic crystal slab defect-waveguide laser with optical pump," *Electron. Lett.*, vol. 39, no. 2, Jan. 23, 2003.

[17] Z.-Y. Li and K.-M. Ho, "Anomalous propagation loss in photonic crystal waveguides," *Phys. Rev. Lett.*, vol. 92, no. 6, p. 063904, 2004.

[18] C. Sauvan and P. Lalanne, "Anomalous propagation loss in photonic crystal waveguides," *Phys. Rev. Lett.*, vol. 95, p. 229401, 2005.

[19] R. S. Jacobsen, A. V. Lavrinenko, L. H. Frandsen, C. Peucheret, B. Zsigri, G. Moulin, J. Fage-Pedersen, and P. I. Borel, "Direct experimental and numerical determination of extremely high group indices in photonic crystal waveguides," *Opt. Exp.*, vol. 13, no. 20, pp. 7861–7871, Oct. 3, 2005.

Martin J. Cryan received the B.Eng. degree in electronic engineering from the University of Leeds, U.K., in 1986, and the Ph.D. degree from the University of Bath, U.K., for work on GaAs MMIC design, in 1995.

He worked in industry for five years as a microwave design engineer. From 1994 to 1997, he was a researcher at the University of Birmingham, U.K., where he worked on active integrated antennas. From 1997 to 1999, he was a European Union Training and Mobility of Researchers research fellow working at the University of Perugia, Italy, on the design and simulation of quasi-optical multipliers using the Lumped—Element FDTD method. From 2000 to 2002, he was a research associate at the University of Bristol, U.K., working on hybrid electromagnetic methods for EMC problems in optical transceivers and FDTD analysis of photonic crystals. He was appointed as a Lecturer in the Department of Electrical and Electronic Engineering, University of Bristol, in 2002 and was made Senior Lecturer in 2007. He has published 35 journal and more than 100 conference papers (eight invited) in the areas of fabrication, modeling and measurement of photonic crystal based devices, radio-over-fibre, active integrated antennas, FDTD analysis, and MMIC design.